Archives of Oral Biology 68 (2016) 105–115

Contents lists available at ScienceDirect

Archives of Oral Biology

journal homepage: www.elsevier.com/locate/aob

DNA methylation profiling in different phases of temporomandibular joint osteoarthritis in rats

Jia-Ling Xiao[a], Juan-Hong Meng[a,*], Ye-Hua Gan[b,**], Ya-Li Li[c], Chun-Yan Zhou[d], Xu-Chen Ma[b]

[a] Department of Oral and Maxillofacial Surgery, Peking University School and Hospital of Stomatology, Beijing 100081, PR China
[b] Center for Temporomandibular Joint Disorder and Orofacial Pain, Peking University School and Hospital of Stomatology, Beijing 100081, PR China
[c] Department of Dermatology and Venereology, Peking University First Hospital, Beijing 100034, PR China
[d] Department of Biochemistry and Molecular Biology, Peking University School of Basic Medical Sciences, Beijing 100191, PR China

ARTICLE INFO

Article history:
Received 14 December 2015
Received in revised form 3 April 2016
Accepted 18 April 2016

Keywords:
Temporomandibular joint
Osteoarthritis
DNA methylation
Claudin11

ABSTRACT

Objective: Temporomandibular joint osteoarthritis (TMJOA) is a complex disease with strong genetic and epigenetic components in its pathogenesis. The aim of this study was to evaluate DNA methylation in mandibular head cartilage in different phases of experimentally-induced TMJOA in rats.
Design: DNA methylation was evaluated using microarrays in the mandibular head cartilage of early, intermediate and late stage experimentally-induced TMJOA, and of the normal age-matched control groups. Genes with differentially methylated CpG sites were analyzed to reveal the over-represented gene ontologies and pathways at different stages, and were compared with published expression profiles to assess their overlappings. The DNA methylation patterns of the target genes were validated by methylated DNA immunoprecipitation qPCR in additional independent cartilage samples and mRNA levels were analyzed by real-time PCR.
Results: We observed 9489 differentially methylated regions between the TMJOA and controls. A total of 440 consistently altered genes were revealed in all three stages; most (80%) were hypomethylated and many were associated with cell cycle regulation. We also detected different DNA methylation changes in early and late stage TMJOA ($R_{early} = 0.68$, $R_{late} = 0.47$), while the differences between age-matched healthy cartilage were subtle. Strong inverse changes between methylation status and mRNA levels were confirmed in *Adamts5*,*Chad, Cldn11* and *Tnf*.
Conclusions: Our data reveals dynamic DNA methylation patterns during the progression of TMJOA, with a different host of genes and pathways. The changes of cartilage DNA methylation patterns might contribute to understand the etiologic mechanisms of TMJOA epigenetically.

1. Introduction

Osteoarthritis (OA) is a common form of temporomandibular disorders (TMD), which results in altered joint structure such as remodeling, articular cartilage abrasion and deterioration, along with changes in the subchondral bone and other soft tissues of the temporomandibular joint (TMJ) (Dijkgraaf, de Bont, & Boering, 1995; Jiao, Niu, & Wang, 2011). OA has a complex and multifactorial etiopathogenesis, with multiple risk factors implicated in its pathogenesis including age, trauma, joint or muscle disturbances, genetics, and systemic conditions (Ikeda, Yonemitsu, & Takei, 2014; Tanaka, Detamore, & Mercuri, 2008). In recent years, epigenetic alterations have been increasingly recognized, generating a new perspective on the pathogenesis of OA (Barter, Bui, & Young, 2012; Reynard & Loughlin, 2012).

DNA methylation, which is the most widely studied epigenetic modification, targets the DNA sequence itself, involving the direct addition of a methyl group to the carbon 5 (C5) position of cytosine and leads to gene silencing (Morgan, Santos, & Green, 2005). This methyl group regulates gene expression by interfering with transcription factor recognition sequences or the transcriptional machinery, or with the cooperation of methyl-CpG binding domain

* Corresponding author at: Department of Oral and Maxillofacial Surgery, Center for Temporomandibular Joint Disorder and Orofacial Pain, Peking University School and Hospital of Stomatology, 22 Zhongguancun South Street, Haidian District, Beijing 100081, PR China.
** Corresponding author at: Center for Temporomandibular Joint Disorder and Orofacial Pain, Peking University School and Hospital of Stomatology, 22 Zhongguancun South Street, Haidian District, Beijing 100081, PR China
E-mail addresses: jhmeng@aliyun.com (J.-H. Meng), kqyehuagan@bjmu.edu.cn (Y.-H. Gan).

http://dx.doi.org/10.1016/j.archoralbio.2016.04.006
0003-9969/

proteins (MBDs) (Schubeler, 2015). These modified sites are usually named CpG islands within high-density CpG regions and are located in the promoter of genes.

DNA methylation patterns undergo changes during development, cell differentiation and in response to environmental stimuli, and therefore playing an important role in mammalian development and other complex diseases (Bergman & Cedar, 2013). For example, the methylation of the *O*-6-methylguanine-DNA methyltransferase (MGMT) promoter in gliomas is a useful predictor of the responsiveness of the tumors to alkylating agents (Esteller, Garcia-Foncillas, & Andion, 2000); the epigenetic silencing of X-linked FHL1 is an independent prognostic factor and could be an adjuvant therapeutic intervention in patients with head and neck squamous cell carcinoma (Cao, Liu, & Xia, 2016). Alterations in DNA methylation have also been observed in OA in association with the deregulation of matrix metalloproteinase 3 (MMP3), MMP9, MMP13, ADAMTs4, Leptin and GDF5 (Cheung, Hashimoto, & Yamada, 2009; Niu, Huang, & Zhao, 2011; Reynard, Bui, & Canty-Laird, 2011; Roach, Yamada, & Cheung, 2005). Moreover, several genome-wide DNA methylation studies in knee and/or hip OA revealed a group of differentially methylated CpG sites and functional enrichment associated with the OA development (Fernandez-Tajes, Soto-Hermida, & Vazquez-Mosquera, 2014; Jeffries, Donica, & Baker, 2014; Rushton, Reynard, & Barter, 2014). Understanding DNA methylation in OA may help develop new strategy to treat OA. However, the role of DNA methylation in TMJOA remains to be fully elucidated. Due to the influence of occlusal factor, masticatory muscles and psychological states, the pathogenesis of TMJOA is highly complex, and its epigenetics may be different from those of general OA (Kalladka, Quek, & Heir, 2014).

In the present study, we performed a genome-scale analysis of DNA methylation in the rat mandibular head cartilage of three different stages of experimentally-induced TMJOA and age-matched healthy control TMJ. A group of genes with differential DNA methylation was observed in TMJOA and their potential roles are discussed.

2. Materials and methods

2.1. Animal model and pathological examination

All the animal experiments were approved by the Peking University Institutional Animal Care and Use Committee (No.: LA2012-24). Two-month old male Wistar rats (200–220 g) were anesthetized with the intraperitoneal injection of sodium pentobarbital (50 mg/kg), combining with local infiltration anesthesia by 2% lidocaine during the operation. The TMJOA animal model was created by one-third resection of the anterolateral disc in every left joint and the wound was closed in layers under aseptic conditions as described in detail in previous studies (Lekkas, Honee, & van den Hooff, 1988). Penicillin was administered to prevent post-surgical infection (100,000 units). As no histopathological differences between non-operated controls and sham controls, age-matched rats without surgical intervention on either side of the TMJ were used as normal controls (Meng, Ma, & Ma, 2005). The rats were fed a normal diet for the following experiments.

With 4 TMJOA rats and 2 control rats for each group, a total of 36 rats were sacrificed by sodium pentobarbital overdose (>80 mg/kg) at 2, 4, 6, 8, 12 and 16 weeks postoperatively for the pathological examinations (see online Supplementary Table 1). The TMJ condyles were removed and fixed in 4% paraformaldehyde solution (pH 7.4) and demineralized for one month in 15% EDTA. The 4-μm sections were stained with hematoxylin, eosin and toluidine blue. The pathological grades of TMJOA were determined according to the classifications described by Dijkgraaf et al. (1995).

2.2. Nucleic acid isolation

With 12 TMJOA rats and 12 age-matched healthy control rats for each time-point, the mandibular head of the condylar process of all 72 rats were removed at 4, 8 and 16 weeks for DNA methylation analysis. The cartilage of the mandibular head was carefully separated from the underlying bone, and rapidly submerged in liquid nitrogen. Genomic DNA and total RNA were extracted from different groups of rats mandibular head cartilage using the QIAamp DNA mini kit (QIAGEN, Hilden, Germany), and RNeasy Mini Kit (QIAGEN), respectively. Their concentrations were measured using the NanoDrop 2000c spectrophotometer (Thermo Fisher Scientific, Waltham, MA, USA), and the genomic DNA was also examined by 0.8% agarose gel electrophoresis to ensure its integrity and quality. At least 5 μg genomic DNA was required for each sample to ensure the success of subsequent methylated DNA immunoprecipitation chip (MeDIP-Chip) analyses. Another three groups of DNA and RNA were extracted for the validation of DNA methylation changes and mRNA levels.

2.3. DNA methylation profiling

Genome-scale DNA methylation profiling was performed using Rat DNA Methylation 3 × 720 K Promoter Plus CpG Island Arrays (NimbleGen, Basel, Switzerland), which is a multiplex slide with three identical arrays per slide; each array contains 15,790CpG Islands annotated according to the University of California Santa Cruz (UCSC) Genome Browser Database and 15,287 well-characterized RefSeq promoter regions (located from approximately −3880 bp to +970 base pairs (bp) of the transcriptional start sites) covered by a total of approximately 720,000 probes. After quality control, genomic DNA samples were sonicated to form random fragments (approximately 200–1000 base bp), and methylated DNA was immunoprecipitated using Biomag^{TM} magnetic beads conjugate with a mouse monoclonal antibody against 5-methylcytidine. The total input and immunoprecipitated DNA were labelled with Cy3- and Cy5-labelled random 9-mers, respectively, and hybridized to the microarrays. Scanning was performed with the Axon GenePix 4000B microarray scanner (Axon 132 Instruments, Foster City, CA, USA). All the raw data were subjected to Median-centering, quantile normalisation and linear smoothing using the Bioconductor packages Ringo, limma and MEDME (Palmke, Santacruz, & Walter, 2011; Pelizzola, Koga, & Urban, 2008; Ritchie, Phipson, & Wu, 2015; Toedling, Skylar, & Krueger, 2007). The normalized $\log^2$-ratio data were generated for further peak-finding analysis.

2.4. Data analysis

Region of interest (ROI) analysis was conducted by calculating the mean log2-ratio of the corresponding probes covering defined promoters or CpG islands to evaluate the enrichment or enrichment differences between the TMJOA and control groups. The numbers of differential enrichment peaks (DEP) were also calculated according to every log2-ratio value using M′ method (Palmke et al., 2011). The defined promoters were subdivided into the following three classes based on CpG ratio, GC content and CpG-rich region length: high-CpG-density promoter (HCP), low-CpG-density (LCP), and intermediate-CpG-density (ICP). Correlation Matrix analysis, which is an independent function analysis, was conducted by analyzing raw log2-(IP/Input) values in R, to evaluate the overall correlations of promoters and CpG islands in different stages (Palmke et al., 2011). To reveal the overlappings of differentially methylated genes between different time-point groups, the Venny software was used to generate Venn diagrams (http://bioinfogp.cnb.csic.es/tools/venny/index.html.). Using the

440 selected genes representing the most consistent differentially methylated results, the hierarchical clustering analysis was performed to distinguish different groups. For the unsupervised clustering, distances between the samples was measured based on the Euclidean distance and clustered using the Ward method. DNA methylation profiles in the early and late stages were also selected to compare with our previously published expression microarrays data (Meng et al., 2005).

2.5. Gene ontology analysis

The DAVID (Database for Annotation, Visualization and Integrated Discovery) web server (http://david.abcc.ncifcrf.gov/) was used to perform functional enrichment analysis of gene ontology (GO) and KEGG pathway categories (Huang da et al., 2009). Genes with differentially methylated regions in their promoters and CpG islands were mapped to their respective rat orthologs and then submitted to DAVID for enrichment analysis, which included GO biological processes (GO-BP), cellular component (GO-CC), molecular function (GO-MF) and KEGG pathway categories. For GO-BP, GO-CC, GO-MF or KEGG pathway terms, *P*-value of less than 0.01 were considered to be statistically significant and were, therefore, included in the results.

2.6. Validation

Part of genes were selected for the validation of mRNA expression and DNA methylation changes by real-time PCR and methylated DNA immunoprecipitation qPCR (MeDIP-qPCR), respectively (Weber, Davies, & Wittig, 2005). The significance level was set to 0.05 with one-way analysis of variance (ANOVA).

3. Results

3.1. Histopathological examination

The mandibular head cartilage in control groups had a smooth, intact superficial zone, regular alignment of multilayer chondrocytes, and abundant proteoglycan staining in the mid and deep zones, whereas the cartilage in the experimental groups showed swelling, hyperplasia, irregular arrangement and uneven proteoglycan staining at 4 weeks, thickened cartilage, discontinuity and regional loss of chondrocytes, horizontal splitting, cluster formation and loss proteoglycan staining at 8 weeks, and extensive fibrillation, severe structural disorganization and extensive loss of proteoglycan staining at 16 weeks (Fig. 1A–H). The histopathological changes of the mandibular head cartilage at 4, 8 and 16 weeks postoperatively corresponded to the early, intermediate and late stages of TMJOA (Dijkgraaf et al., 1995); therefore, the genomic DNA of the cartilage of TMJOA groups at these three time-points was extracted to investigate the changes in DNA methylation during the progression of TMJOA.

3.2. Global DNA methylation pattern

In the ROI analysis, a total of 9489 differentially methylated regions were identified in the three osteoarthritic TMJ cartilage samples compared with the control TMJ cartilage samples

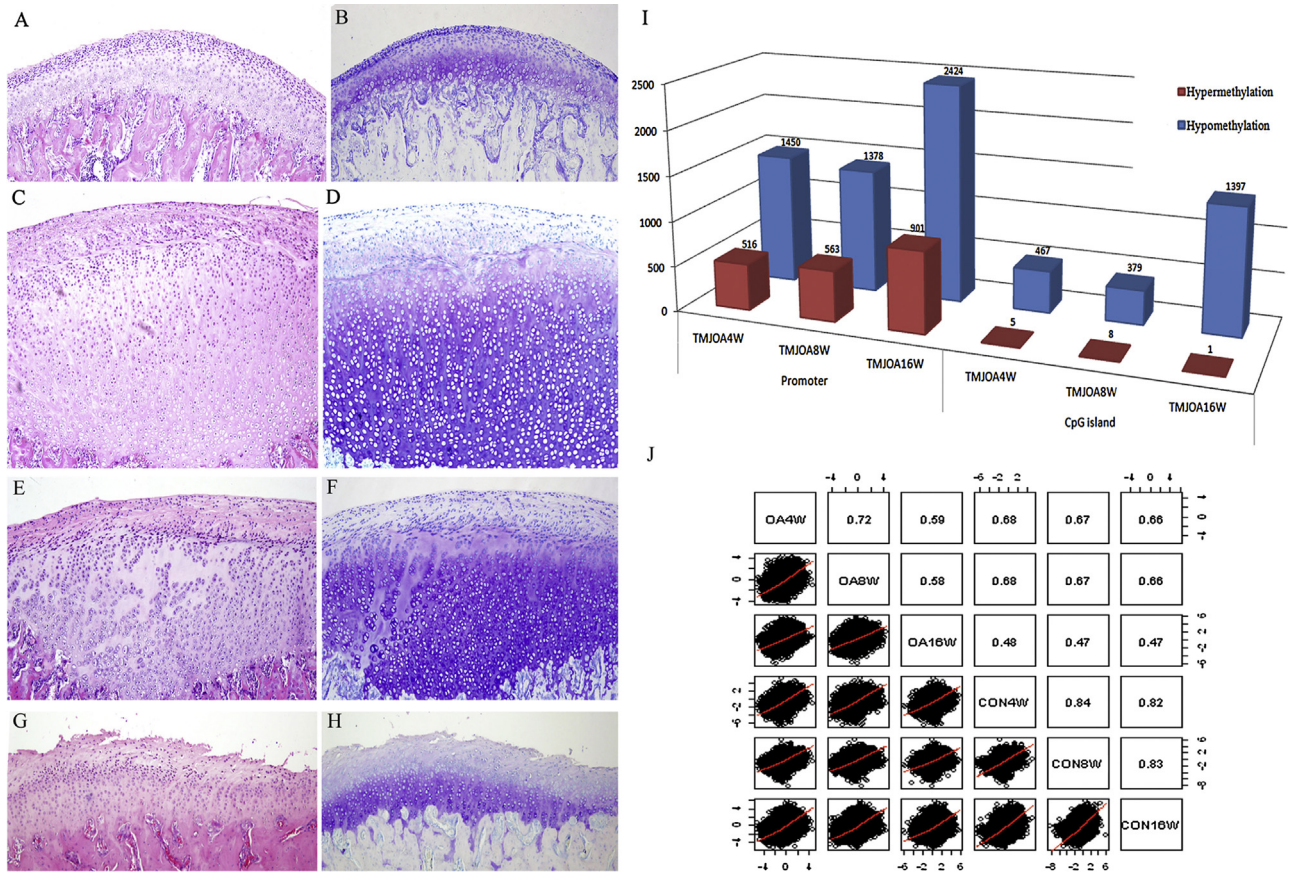

Fig. 1. Histological grades, correlation matrix and global distributions for temporomandibular joint osteoarthritis (TMJOA) and normal controls. (A, B) Staining in normal adult TMJ cartilage; (C, D) staining in early stage TMJOA; (E, F) staining in intermediate stage TMJOA; (G, H) staining in late stage TMJOA; (I) global distributions of differentially methylated regions in the three stages. (J) Correlations matrix revealing the overall correlations between different TMJOA stages and controls; (A, C, E, G) hematoxylin & eosin staining × 100; (B, D, F, H) toluidine blue staining; magnification, ×100).

(Supplementary Table 3). Among them, most (76%) were located in the promoter regions, while 24% were detected in the other CpG islands. Both in the promoters and CpG islands, the number of hypomethylated regions greatly exceeded the number of hypermethylated regions. Furthermore, a markedly greater number of regions were detected in the late stage compared with those in the early and intermediate stages (Fig. 1I). The DNA methylation status were stable among the normal control TMJ cartilage samples at different ages ($R_{4w/8w} = 0.84$, $R_{4w/16w} = 0.82$, $R_{8w/16w} = 0.83$), whereas the correlations of DNA methylation within the three stages of TMJOA cartilage samples was uneven ($R_{4w/8w} = 0.72$, $R_{4w/16w} = 0.59$, $R_{8w/16w} = 0.58$). The correlation of DNA methylation between late

Table 1
Examples of mandibular head cartilage genes harboring differentially methylated regions in all three stages of temporomandibular joint osteoarthritis (TMJOA) compared with age-matched controls ($P < 0.05$).

Gene ID	Gene symbol	Difference in 4 weeks (OA-Con)	Difference in 8 weeks (OA-Con)	Difference in 16 weeks (OA-Con)	Protein Name
Hypomethylation					
81647	ATF2	−0.638	−0.523	−0.610	cyclic AMP-dependent transcription factor ATF-2
79257	AXIN1	−0.889	−0.519	−0.486	axin-1
25296	BMP4	−0.414	−0.783	−0.586	bone morphogenetic protein 4 precursor
361662	BUB3	−0.430	−0.570	−0.932	budding uninhibited by benzimidazoles 3 homolog
83628	CD82	−0.647	−0.499	−0.804	CD82 antigen
360621	CDC6	−0.342	−0.388	−1.132	cell division control protein 6 homolog
305984	CDCA2	−0.419	−0.276	−0.494	cell division cycle-associated protein 2
304407	CLDN4	−0.716	−0.471	−0.790	claudin-4
65132	CLDN7	−0.469	−0.621	−1.148	claudin-7
301012	COL7A1	−0.617	−0.432	−0.559	procollagen, type VII, alpha 1
690300	COX11	−0.477	−0.411	−0.729	COX11 homolog, cytochrome c oxidase assembly
29507	COX7A2	−0.858	−0.796	−1.219	cytochrome c oxidase subunit 7A2, mitochondrial
303251	DVL2	−0.707	−0.634	−0.891	dishevelled 2
25149	ESR2	−0.569	−0.531	−0.664	estrogen receptor beta
299626	GADD45B	−0.428	−0.663	−0.597	growth arrest and DNA damage-inducible protein
291005	GADD45G	−0.426	−0.349	−0.676	growth arrest and DNA damage-inducible protein
25587	ID2	−0.380	−0.398	−0.821	DNA-binding protein inhibitor ID-2
303477	IGF2BP1	−0.457	−0.230	−0.725	insulin-like growth factor 2 mRNA-binding
288905	IL27RA	−0.491	−0.473	−0.821	interleukin-27 receptor subunit alpha
25647	IL7	−0.586	−0.422	−0.576	interleukin-7 precursor
297176	MAD2L1	−0.641	−0.774	−1.430	mitotic spindle assembly checkpoint protein
29279	MEOX2	−0.901	−0.477	−0.742	homeobox protein MOX-2
305897	NFATC4	−0.685	−0.573	−1.017	nuclear factor of activated T-cells, cytoplasmic
294790	SKP2	−0.378	−0.440	−0.449	S-phase kinase-associated protein 2
312936	SOX17	−0.632	−0.470	−0.568	transcription factor SOX-17
311786	TRAF2	−0.469	−0.361	−0.807	TNF receptor-associated factor 2
Hypermethylation					
689404	AMTN	0.817	0.557	1.169	amelotin precursor
302666	ASB11	0.485	0.488	0.603	ankyrin repeat and SOCS box protein 11
294560	CCDC109A	0.478	0.480	0.733	coiled-coil domain-containing protein 109A
81645	CHRM2	0.363	0.606	0.570	muscarinic acetylcholine receptor M2
497840	CPS1	0.519	0.510	0.630	carbamoyl-phosphate synthase [ammonia],
29298	CYP2C7	0.792	1.251	0.993	cytochrome P450 2C7
361944	ELF2	0.052	0.767	0.907	E74-like factor 2 isoform 2
84488	FGF13	0.891	0.595	0.814	fibroblast growth factor 13
54257	GRIK2	0.914	1.016	0.740	glutamate receptor, ionotropic kainate 2
494500	GSTA5	0.357	0.435	0.447	glutathione S-transferase alpha-5
502359	HBE2	0.481	0.689	0.803	hemoglobin, epsilon 2
24476	IAPP	0.688	0.468	0.553	islet amyloid polypeptide precursor
311783	IL1F5	0.470	0.960	0.880	interleukin-1 family member 5
450225	KRT10	0.459	0.536	0.713	keratin, type I cytoskeletal 10
65146	LILRB3	0.724	0.538	0.544	leukocyte immunoglobulin-like receptor,
317270	MAGEB18	0.968	0.527	1.205	melanoma-associated antigen B18
29152	MSTN	0.842	0.716	0.854	growth/differentiation factor 8 precursor
288866	OLR1057	0.753	1.161	0.508	olfactory receptor Olr1057
293245	OLR106	0.661	0.508	1.075	olfactory receptor Olr106
300392	OLR1124	0.555	0.666	0.840	olfactory receptor Olr1124
405164	OLR1166	0.505	1.024	0.550	olfactory receptor Olr1166
310630	SEMA4A	0.523	0.588	0.735	semaphorin-4A
497756	SI	0.621	0.530	0.808	sucrase-isomaltase, intestinal
291060	SNRNP48	0.548	0.304	0.573	U11/U12 small nuclear ribonucleoprotein 48 kDa
64555	SPEF2	0.388	0.441	0.579	sperm flagellar protein 2
362267	SVS6	0.755	0.647	1.080	seminal vesicle secretory protein 6

stage TMJOA with its corresponding control group was much lower than the other two ($R_{16w} = 0.47$, $P < 0.001$). These data suggested that the differences in DNA methylation status between the TMJOA groups and the corresponding control groups increased with TMJOA progression (Fig. 1J).

3.3. Characterization of consistently differentially methylated genes

Venn analysis revealed the overlapping sections of DNA methylation profiles at different stages of TMJOA (data not shown). A total of 469 genes were differentially methylated at all early, intermediate and late stages of TMJOA. With the exception of 29 genes with inconsistent DNA methylation changes, the remaining 440 genes exhibited the most consistently differential methylation patterns (369 hypomethylated and 71 hypermethylated; key examples and the full list are shown in Table 1, and Supplementary Table 5, respectively). Unsupervised clustering analysis showed clear separation of the TMJOA and control groups on the basis of the methylation profile of these 440 genes (Fig. 2A, hierarchical analysis for all differentially methylated genes is shown in Supplementary Fig. 1). GO analysis of the 369 hypomethylated genes indicated an enrichment of biological processes related to cell cycle regulation ($P = 0.0004$) (data not shown), including *Gadd45b, Gadd45 g, Id2, Cdc6, Skp2, Bub3*, and *Mad2l1*. A subsection of the hypomethylated genes was also involved in the anabolic or catabolic pathways of cartilage homeostasis (including *Bmp4, Igf2bp1, Col7a1, Atf2, Axin1, Fgf13*), and immune responses (including *Il7, Il27ra, Traf2* and *Nfatc4*). Notably, the important components of tight junctions, claudin 4 (*Cldn4*), *Cldn7* and *Cldn11*, were identified as significantly hypomethylated, and their gene expressions were also validated to be upregulated in both early and late stages of TMJOA. Nevertheless, few of the hypermethylated genes exhibited a relationship with TMJOA, including a large group of genes associated with detection of chemical stimuli or the olfactory receptor family genes.

3.4. Analysis of differentially methylated genes in the early or late stage

Analysis of the DNA methylation profiles in the early stage TMJOA compared with control group revealed a total of 2198 differentially methylated genes (1681 hypomethylated and 517 hypermethylated). GO and KEGG pathway analyses indicated enrichment of biological processes involved in the early stage (examples shown in Table 2 and Fig. 2B), especially the processes involving in cell cycle regulation ($P < 0.001$), the immune response ($P = 0.0027$) and intracellular signaling cascades ($P = 0.008$). Those related to inflammation or immune responses, such as tumor necrosis factor (*Tnf*), *Tnfrsf1a*, *Traf2*, *Il7*, *Il2ra*, *Il4ra*, *Il9ra*, and *Il27ra*, and those associated with the ECM degradation, such as *Adamts5*, *Adamtsl5*, and *Adam1a*, showed significantly decreased DNA methylation. Part results were verified by analysis of the mRNA levels such as *Tnf*, an important inflammatory cytokine usually overexpressed in TMJOA patients, (early stage 2.51 ± 0.42, late stage 2.64 ± 0.41, $P = 0.002$), and *Adamts5*, one of the major aggrecanases leading to cartilage degradation (early 3.25 ± 0.24, late 3.06 ± 1.18, $P = 0.013$). In addition, the runt-related transcription factor 1 (*Runx1*), previously identified as the most differentially methylated gene in both knee and hip OA (Fernandez-Tajes et al., 2014; Jeffries et al., 2014), was also found to be differentially methylated in the early and late stages of TMJOA in our study.

At the late stage, a total of 3960 differentially methylated genes were detected (3061 hypomethylated and 899 hypermethylated), a majority (60%) of which were identified in the late stage alone. Besides the genes associated with ECM degradation or the immune response, such as *Adamts* and *Ils*, which were also identified in the

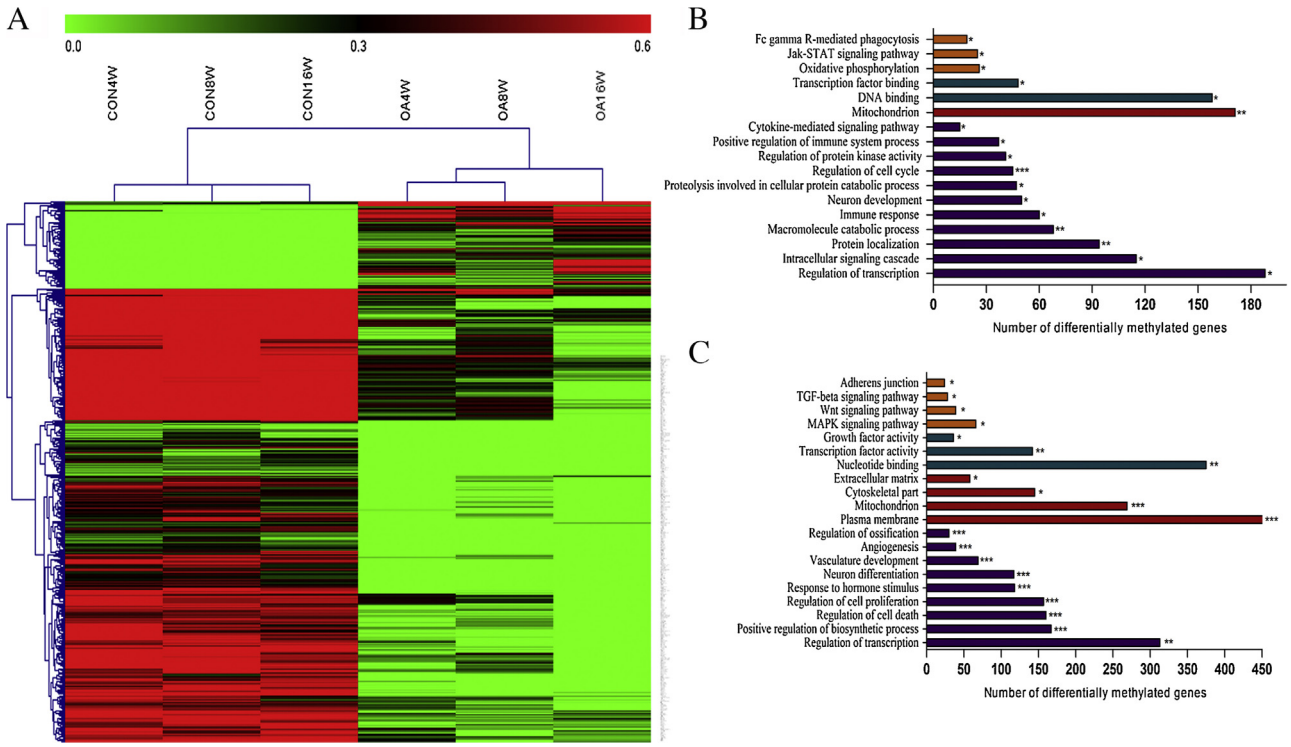

Fig. 2. Hierarchical analysis of consistently altered genes and representative functional categories in early and late stage temporomandibular joint osteoarthritis (TMJOA). (A) Heatmap showing the most consistent differentially methylated genes in all three stages; (B, C) the most relevant functional categories of early and late TMJOA identified by GO and KEGG pathway analysis. $^{*}P \leq 0.01$, $^{**}P \leq 0.001$, $^{***}P \leq 0.0001$ determined with a modified Fisher's exact test.

Table 2
Examples of mandibular head cartilage genes harboring differentially methylated regions sorted by decreased DNA methylation differences in temporomandibular joint osteoarthritis (TMJOA) compared with age-matched controls.

Early stage of TMJOA						Late stage of TMJOA					
Gene	Chr.	DNA methylation in TMJOA4w	DNA methylation in Con4w	Difference in 4w (TMJOA-Con)	P value	Gene	Chr.	DNA methylation in TMJOA16w	DNA methylation in Con16w	Difference in 16w (TMJOA-Con)	P value
IL9R	chr10	0.168	1.189	−1.021	7.81E-03	JUN	chr5	−0.152	0.857	−1.009	1.95E-03
AXIN1	chr10	−0.128	0.761	−0.889	7.81E-03	ADAMTSL5	chr7	−0.126	0.833	−0.959	2.44E-04
TNFRSF1A	chr4	−0.333	0.544	−0.878	3.91E-03	PDGFB	chr7	0.349	1.289	−0.940	1.95E-03
TNFAIP1	chr10	−0.162	0.618	−0.780	7.81E-03	ANGPTL4	chr7	−0.412	0.507	−0.920	3.91E-03
DKK1	chr1	−0.349	0.345	−0.694	7.81E-03	CTGF	chr1	0.037	0.912	−0.876	4.69E-02
ECM1	chr2	−0.143	0.525	−0.667	5.86E-03	MAP3K7	chr5	0.245	1.092	−0.847	1.56E-02
BMPER	chr8	−0.204	0.446	−0.650	2.73E-02	WNT1	chr7	−0.024	0.810	−0.834	3.91E-03
ADAMTS5	chr11	0.046	0.685	−0.640	7.81E-03	IL27RA	chr19	−0.566	0.254	−0.821	7.81E-03
COL7A1	chr8	0.062	0.679	−0.617	2.73E-02	SFRP2	chr2	0.327	1.144	−0.817	9.77E-04
ADAMTSL5	chr7	0.105	0.692	−0.588	9.77E-03	ACVR2B	chr8	0.388	1.202	−0.813	3.91E-03
IL7	chr2	0.310	0.895	−0.586	1.95E-03	ERK2	chr11	−0.455	0.335	−0.790	3.91E-03
RUNX1	chr11	0.277	0.854	−0.577	7.63E-03	VEGFA	chr9	−0.249	0.540	−0.790	3.91E-03
IL2RA	chr17	−0.446	0.101	−0.547	5.86E-03	PDGFA	chr12	0.393	1.166	−0.773	7.63E-06
SMAD5	chr17	−0.413	0.120	−0.533	3.91E-03	WNT16	chr4	−0.070	0.699	−0.769	3.91E-03
TNF	chr9	−0.359	0.144	−0.503	3.91E-03	SMAD7	chr18	0.334	1.077	−0.743	1.33E-05
IL27RA	chr19	−0.177	0.315	−0.491	7.81E-03	TNF	chr9	−0.651	0.073	−0.724	3.91E-03
IGF2BP1	chr10	−0.025	0.432	−0.457	3.91E-03	WNT5B	chr4	−0.292	0.410	−0.703	3.91E-03
WNT8A	chr18	0.164	0.614	−0.451	4.88E-02	ECM1	chr2	−0.143	0.525	−0.667	5.86E-03
COL1A2	chr4	0.282	0.701	−0.419	1.37E-02	RUNX1	chr11	0.186	0.848	−0.663	6.10E-05
IL20RA	chr1	−0.075	0.339	−0.414	3.91E-03	FGFR1	chr16	0.219	0.869	−0.649	1.56E-02
BMP4	chr15	0.099	0.513	−0.414	3.71E-02	AXIN2	chr10	−0.319	0.315	−0.634	1.95E-02
SMAD6	chr8	0.180	0.518	−0.338	2.73E-02	FGF1	chr18	−0.222	0.378	−0.601	9.77E-03
COL8A1	chr11	0.146	0.460	−0.314	3.91E-02	TGFB2	chr13	0.027	0.622	−0.596	4.88E-02
ADAM1A	chr12	0.274	0.567	−0.293	3.91E-03	MMP28	chr10	0.340	0.925	−0.585	3.71E-02
IL4RA	chr1	0.043	0.335	−0.291	3.91E-03	BMP4	chr15	0.097	0.679	−0.582	3.81E-05
BMPR1A	chr16	0.464	−0.079	0.543	3.91E-03	IL7	chr2	0.151	0.728	−0.576	3.71E-02
RUNX2	chr9	0.029	−0.368	0.397	2.73E-02	MMP8	chr8	−0.242	0.326	−0.568	1.37E-02
						COL1A2	chr4	0.215	0.762	−0.547	9.77E-03
						TGFB1	chr1	−0.058	0.484	−0.542	1.56E-02
						MAP4K2	chr1	0.315	0.854	−0.539	2.73E-02
						TNFRSF1B	chr5	0.005	0.530	−0.525	9.77E-03
						AXIN1	chr10	0.075	0.561	−0.486	7.81E-03
						MMP14	chr15	−0.458	0.010	−0.468	1.37E-02
						TGFBR2	chr8	−0.042	0.393	−0.436	3.91E-02
						ADAMTS15	chr8	0.257	0.643	−0.385	1.17E-02

Table 2 (*Continued*)

Early stage of TMJOA						Late stage of TMJOA					
Gene	Chr.	DNA methylation in TMJOA4w	DNA methylation in Con4w	Difference in 4w (TMJOA-Con)	P value	Gene	Chr.	DNA methylation in TMJOA16w	DNA methylation in Con16w	Difference in 16w (TMJOA-Con)	P value
						COL27A1	chr5	0.294	0.648	−0.354	6.94E-04
						WNT5A	chr16	0.270	0.589	−0.319	2.34E-02
						MEK4	chr10	0.038	0.344	−0.306	1.95E-02
						SMAD4	chr18	0.372	−0.432	0.804	3.91E-03
						PRG4	chr13	0.208	−0.462	0.670	1.95E-02
						MEPE	chr14	0.404	−0.065	0.470	4.88E-02
						OMD	chr17	0.270	−0.122	0.392	2.73E-02
						AKT3	chr13	0.073	−0.278	0.351	3.91E-02

early stage, further groups of biological processes and pathways were identified in the late stage. These were predominantly the TGFβ signaling pathway ($P = 0.0014$) including *Tgfb1*, *Tgfb2*, *Tgfbr2*, *Acvr2b*, *Smad4*, and *Smad7*, the MAPK signaling pathway ($P = 0.0031$) including *Mapk1* (*Erk2*), *Map2k4* (*Mek4*), *Map4k2*, *Map3k7* (*Tak1*), and *Map3k13*, angiogenesis or vasculature development ($P < 0.0001$) including vascular endothelial growth factor a (*Vegfa*), *Ctgf*, *Fgfr1*, *Fgf1*, *Pdgfa*, *Pdgfb*, *Angptl4*, and *Akt3*, and regulation of ossification ($P < 0.0001$) including *Omd*, *Mepe* (Fig. 2C). In the late stage, we also identified a group of genes associated with the ECM of articular cartilage ($P = 0.007$), including *Ecm1*, *Col1a2*, *Col27a1*, *Col4a4*, and *Prg4* (examples shown in Table 2).

3.5. Comparative analysis and further validation

An integrated analysis of the results of DNA methylation assays with those obtained in our previous mRNA expression assays in TMJOA revealed an inverse changes between DNA methylation and mRNA expression of 62 genes (25 genes in the early stage and 37 in the late stage). A total of 56 genes were hypomethylated in DNA methylation array, and also upregulated in the mRNA expression array. In particular, chondroadherin (*Chad*), mesenchyme homeobox 2 (*Meox2*), and inhibitor of DNA binding 2 (*Id2*) were found to be significantly hypomethylated and overexpressed both in the early and late stage TMJOA array analyses (Table 3).

Based on the ROI and DEP analysis and the comparison with the results of our previous expression microarray analyses, the five genes (*Chad*, *Cldn11*, *Meox2*, *Id2* and cadherin 2 (*Cdh2*)), which showed significantly differential DNA methylation in early and late stage TMJOA and had over 2-fold changes in expression microarray, were selected to verify the alterations in the independent TMJOA samples (Supplementary Table 4). Several functional genes (*Adamts5*, *Tnf* and *Adamtsl5*) associated with extracellular matrix (ECM) degradation or involved in inflammation or immunity were also included in the validation. The mRNA expression and changes in DNA methylation of these genes were confirmed by real-time PCR and MeDIP-qPCR, respectively, with the exception of the DNA methylation changes for *Meox2* and *Cdh2* (Fig. 3). Notably, we found a significant upregulation of *Chad* mRNA expression compared with the control (early 2.85 ± 0.29, late 8.77 ± 1.00, $P = 9.852e\text{-}06$) and its hypomethylation status was also confirmed as compared with the control (early 0.28 ± 0.04, late 0.215 ± 0.233, $P = 0.010$). Among the tight junction-associated genes, the hypomethylated *Cldn11* was found to correlate with the most significant mRNA upregulation, as compared with the controls (early 95.67 ± 24.83, late 7.26 ± 0.90, $P = 3.196e\text{-}4$). Furthermore, the upregulations of *Adamts5* and *Tnf* in different stages of TMJOA were also consistent with their DNA methylation changes ($R^2_{Adamts5} = 0.997$, $R^2_{Tnf} = 0.827$).

4. Discussion

In this study, we generated genome-scale DNA methylation profiles from the mandibular head cartilage in the early, intermediate and late phases of an experimentally-induced model of TMJOA in rats. We also compared the current DNA methylation array analysis results with those obtained in our previous transcriptome studies. The changes in DNA methylation and mRNA expression of the most consistently differentially expressed genes were confirmed in a further independent TMJOA cartilage samples. The differentially methylated pathways and genes dynamically changed with the progression of experimental TMJOA. Our results suggested that the epigenetic events would play an important role in the progression of TMJOA, and that future clinical intervention on DNA methylation would be a new strategy of preventing progression of TMJOA.

In the present study, we provide a unique insight into the progression of TMJOA, and reveal distinct differences in the DNA methylation patterns of differentially expressed genes in the mandibular head cartilage at different stages of TMJOA by comparison with the control groups, whereas, only subtle differences were found between the patterns observed in the cartilage samples obtained from age-matched healthy animals. Specifically, our analysis revealed an enrichment of immune response and regulation of cell cycle genes in the early stage of TMJOA, while in the late stage there was enrichment of angiogenesis-related genes, such as *Vegfa, Ctgf*, and those associated with regulation of ossification, such as *Mepe*, *Omd*, both of which are associated with the invasion of articular cartilage by blood vessels and advancing endochondral ossification (Nampei, Hashimoto, & Hayashida, 2004; Ramasamy, Kusumbe, & Wang, 2014). The TGF-β, MAPK and Wnt signaling pathways were also found to be enriched, which is consistent the cross-talk of the MAPK-MMP pathways, which are

Table 3
List of significantly altered genes showing an inverse alteration between DNA methylation and mRNA expression level in early and late stage TMJOA and sorted by decreased expression differences ($P \leq 0.05$).

Early stage of TMJOA								Late stage of TMJOA							
Gene symbol	Chr.	Promoter Classfication	Diff. for DM (EOA-Co)	Diff. for DM (MOA-Co)	Diff. for DM (LOA-Co)	Diff. for expression (EOA / Co)	Diff. for expression (LOA / Co)	Gene symbol	Chr.	Promoter Classfication	Diff for DM (EOA-Co)	Diff for DM (MOA-Co)	Diff for DM (LOA-Co)	Diff for expression (EOA/Co)	Diff for expression (LOA/Co)
CHAD	chr10	ICP	−0.600	−0.013	−0.688	2.85	4.54	MEOX2	chr6	ICP	−0.901	−0.477	−0.742	2.56	5.17
MEOX2	chr6	ICP	−0.901	−0.477	−0.742	2.56	5.17	CLDN11	chr2	HCP	0.012	0.002	−0.684	2.64	5.07
CSDA	chr4	HCP	−0.509	−0.718	−0.753	1.92	1.57	CHAD	chr10	ICP	−0.600	−0.013	−0.688	2.85	4.54
GOT2	chr19	HCP	−0.468	−0.779	−0.629	1.51	1.16	CASR	chr11	ICP	−0.193	−0.227	−0.751	1.65	4.27
ID2	chr6	ICP	−0.380	−0.398	−0.821	1.31	1.63	GDA	chr1	ICP	−0.055	0.064	−0.382	2.08	2.71
RPS29	chr6	HCP	−0.500	−0.251	−0.630	1.26	1.32	NOV	chr7	ICP	−0.011	−0.043	−0.644	1.58	2.44
LDHA	chr1	HCP	−0.476	−0.525	−0.394	1.26	1.28	PRRX2	chr3	HCP	−0.284	−0.451	−0.762	1.21	2.38
BNIP3	chr1	HCP	−0.738	−0.353	−0.925	1.24	1.69	PLAT	chr16	ICP	−0.428	−0.510	−0.727	1.16	2.33
GNB2L1	chr10	HCP	−0.534	−0.428	−0.488	1.24	1.21	WISP2	chr3	LCP	−0.199	−0.161	−0.667	1.58	2.08
CAST	chr2	ICP	−0.258	0.186	−0.150	1.23	1.49	GNG8	chr1	LCP	0.118	−0.058	−0.377	1.31	1.76
RAB26	chr10	LCP	−0.819	−0.674	−0.424	1.22	1.45	FZD1	chr4	HCP	−0.107	−0.082	−0.383	1.46	1.76
UGT1A6	chr9	LCP	−0.445	−0.150	−0.397	1.21	0.80	RNASE4	chr15	ICP	−0.129	−0.388	−1.038	1.18	1.71
DUOX2	chr3	ICP	−0.385	−0.438	−0.850	1.18	1.24	ENO2	chr4	LCP	−0.202	−0.740	−0.491	1.12	1.70
PPP2R5B	chr1	LCP	−0.781	−0.252	−1.030	1.17	1.29	ANXA4	chr4	ICP	−0.605	−0.696	−0.920	1.29	1.69
EPHX2	chr15	ICP	−0.454	−0.133	−0.105	1.15	1.12	BNIP3	chr1	HCP	−0.738	−0.353	−0.925	1.24	1.69
GNB2	chr12	HCP	−0.601	−0.204	−0.007	1.14	1.28	CANX	chr10	HCP	−0.373	−0.029	−1.011	1.17	1.66
RPL28	chr1	HCP	−0.704	−0.319	−0.226	1.12	1.11	PCDHGC3	chr18	HCP	−0.489	−0.717	−0.828	1.02	1.65
NUPR1	chr1	LCP	−0.475	−0.740	−0.638	1.11	1.35	CTF1	chr1	LCP	−0.422	−0.141	−0.481	1.29	1.63
COLEC12	chr18	HCP	−0.851	−0.325	−0.766	1.11	1.27	ID2	chr6	ICP	−0.380	−0.398	−0.821	1.31	1.63
OAT	chr1	HCP	−0.327	−0.460	−0.649	1.09	1.35	HK3	chr17	LCP	−0.231	−0.195	−0.432	1.29	1.50
KIF1B	chr5	HCP	−0.467	−0.408	−0.318	1.09	1.43	TPI1	chr4	HCP	−0.654	−0.578	−0.777	1.20	1.45
PCDHGC3	chr18	HCP	−0.489	−0.717	−0.828	0.97	1.19	PMP22	chr10	LCP	0.030	0.330	−0.634	1.20	1.44
TFPI2	chr4	ICP	−0.276	−0.519	−0.402	0.96	0.55	OAT	chr1	HCP	−0.327	−0.460	−0.649	1.09	1.35
LGMN	chr6	LCP	0.674	0.068	−0.032	0.80	0.71	FXYD5	chr1	LCP	−0.135	−0.052	−0.686	1.22	1.35
FKBP1A	chr3	HCP	0.459	0.753	0.534	0.90	0.87	CTSB	chr15	HCP	−0.582	−0.365	−1.172	1.17	1.34
								PPP2R5B	chr1	LCP	−0.781	−0.252	−1.030	1.17	1.29
								COLEC12	chr18	HCP	−0.851	−0.325	−0.766	1.11	1.27
								GNAI3	chr2	HCP	−0.202	−0.502	−0.649	1.14	1.24
								HSD17B1	chr10	LCP	−0.060	−0.525	−1.319	1.13	1.20
								HSD17B10	chrX	ICP	0.054	−0.335	−0.413	1.13	1.20
								CLTB	chr17	HCP	−0.292	−0.231	−0.320	1.11	1.19
								RPS21	chr3	HCP	−0.266	−0.264	−0.738	1.07	1.19
								RPS10	chr20	HCP	0.192	0.249	−0.419	1.06	1.13
								CDH2	chr18	LCP	0.485	0.793	0.618	0.64	0.46
								OMD	chr17	LCP	0.557	0.172	0.392	0.83	0.66
								HEPH	chrX	LCP	0.246	0.424	0.639	0.79	0.68
								MEPE	chr14	ICP	0.069	0.075	0.470	0.93	0.72

DM: differentially methylated; EOA: early stage of TMJOA; MOA: intermediate stage of TMJOA; LOA: late stage of TMJOA.

transcriptionally regulated by classic mediators such as VEGFA, TGFß3, TNF-α and other cytokines (Prasadam, Crawford, & Xiao, 2012), all of which activate a pleiotropic cascade of signaling pathways, and may contribute to the development of late stage TMJOA. Overall, the identifications of pathways enriched in differentially methylated genes between TMJOA and TMJOA-free cartilage highlight etiologic mechanisms involved in the disease, and based on the distinct DNA methylation patterns between TMJOAs and/or controls, DNA methylation might be used as the disease monitoring tool.

Analysis of the DNA methylation pattern in early stage TMJOA revealed significant differential methylation of several genes involved in OA pathogenesis, especially *Tnf*, *Adamts5* and Runx family genes, with concomitant changes in mRNA expression. TNF

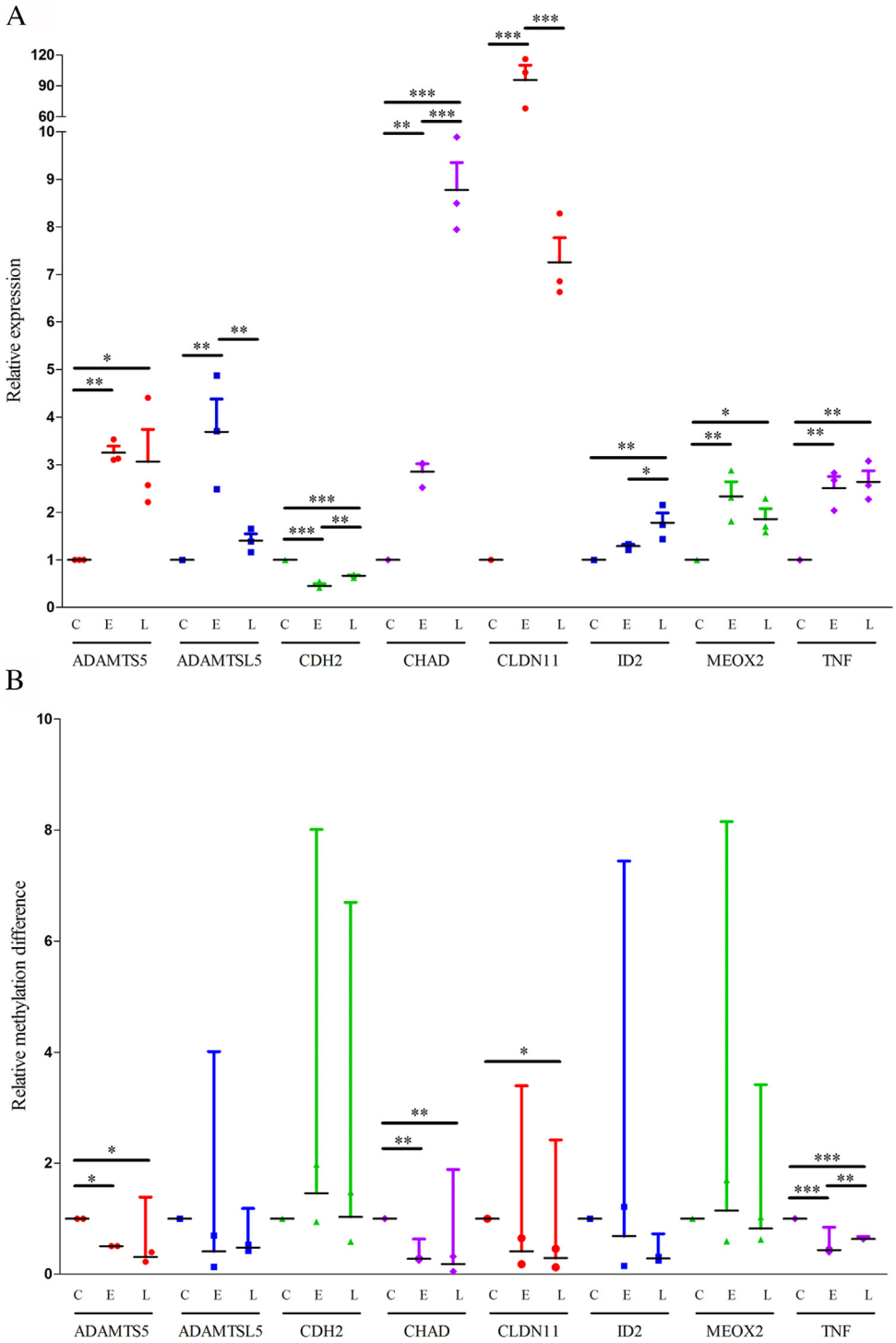

Fig. 3. Validation of target genes by real-time PCR for mRNA expression and MeDIP-qPCR for methylation changes. (A) Real-time PCR analysis of the selected differentially methylated genes in three independent TMJOA cartilage samples. (B) MeDIP-qPCR analysis of the target genes in two independent samples. C = rat cartilage samples of the mandibular head with no surgical operation; E = rat cartilage samples of the mandibular head in the early stage TMJOA; L = rat cartilage samples of the mandibular head in the late stage TMJOA. Values represent means ± 95% confidence interval (95% CI). $^{*}P \leq 0.05$, $^{**}P \leq 0.01$, $^{***}P \leq 0.001$ determined with one-way analysis of variance (ANOVA).

is involved in cellular responses to stimuli, such as cytokines and stress, and is believed to play a pivotal role in the initiation and development of OA (Probert, Akassoglou, & Alexopoulou, 1996). The loss of aggrecan, through the actions of aggrecanase enzymes, is a key event in early OA, with ADAMTS5 identified as one of the major cartilage aggrecanases in osteoarthritic cartilage (Huang & Wu, 2008; Li, Wu, & Jiang, 2014). Thus, both *Tnf* and *Adamts5* are implicated as novel genes regulated by DNA methylation in TMJOA as mentioned in previous hip OA methylation results (Rushton et al., 2014). On the other hand, the Runx family of transcription factors have been characterized as master regulatory factors of chondrogenesis, osteogenesis, hematopoiesis and the differentiation of specific cell phenotypes (Komori, 2005). In accordance with the results of our study of TMJOA, the previous knee and hip OA genome-wide DNA methylation study identified RUNX1 as the most and sixth most hypomethylated CpG sites in their arrays (Fernandez-Tajes et al., 2014; Jeffries et al., 2014). Runx1 is a known inducer of chondrogenic differentiation and a suppressor of subsequent hypertrophy. It is expressed in adult articular cartilage and its expression is downregulated in OA cartilage (Yano, Hojo, & Ohba, 2013). *Runx2,* however, was found to be hypermethylated in the early stage of TMJOA, which is in conflict with the epigenetic alterations identified by Jeffries et al. (2014). Runx2 targets genes including MMPs, growth factors and ECM proteins, that are important for endochondral development, and it is deregulated in chondro-osseous diseases (Komori, 2005). Besides, within the most consistently differentially methylated genes in three stage TMJOA, only five of these genes were identified in the previous knee or hip osteoarthritic methylation studies (ARHGAP9,ARHGEF3, FCGR2A, OAT, PTPN6) (Fernandez-Tajes et al., 2014; Jeffries et al., 2014). Those inconsistent findings indicate TMJ may have different properties with the knee or hip joints. For exmaple, the knee joint is a load-bearing joint, whereas TMJ is a shear-bearing joint; the type of cartilage in the knee or hip joint is hyaline, whereas it is fibrocartilage in TMJ; OA lesions tend to develop mainly in old age in the knee joint, whereas in the TMJ it can be seen in relatively young patients (Gepstein, Shapiro, & Arbel, 2002; Kalladka et al., 2014). Therefore, it is important to further investigate and confirm the epigenetic status and expression patterns of those genes during the TMJOA progression.

Importantly, in this study, we identified a subset of novel genes, especially the claudin (CLDN) family and growth arrest and DNA-damage-inducible 45 (GADD45) family genes, which exhibit highly consistent changes in DNA methylation. CLDN11 is an essential components of tight junctions and plays a role in cell-to-cell interactions or cellular interactions with the ECM that maintain cell adhesion and regulate paracellular transport of ions (Bronstein, Popper, & Micevych, 1996). In early embryonic life, CLDN11 is expressed in the developing meninges and mesenchymal cells, especially around some regions of chondrocyte formation (Bronstein, Chen, & Tiwari-Woodruff, 2000). Other studies have also reported aberrant claudin expression in association with proliferation and migration in various types of cancer. For example, high CLDN4 expression has been reported in pancreatic cancer, while CLDN7 downregulation is observed in head and neck or metastatic breast cancer (Al Moustafa, Alaoui-Jamali, & Batist, 2002; Kominsky, Argani, & Korz, 2003; Nichols, Ashfaq, & Iacobuzio-Donahue, 2004). Furthermore, CpG island hypermethylation in the CLDN11 promoter has been reported in bladder and gastric cancers, and also in dysplastic nevus; this pattern could, therefore, indicate the significance of this gene in the development of these cancers as well as highlighting its potential as an important epigenetic marker in the melanoma development (Agarwal, Mori, & Cheng, 2009; Gao, van den Hurk, & Moerkerk, 2014). In our study, significantly decreased methylation of the *Cldn11* promoter was identified, with a concomitant significant increase in mRNA expression. It can be speculated that dysregulated *Cldn11* expression is involved in the intracellular signaling that controls the proliferation, hypertrophy or disorganization of chondrocytes during TMJOA and deserves further investigation. Moreover, the detection of hypomethylation of two other claudin family genes, *Cldn4* and *Cldn7*, indicates that three genes might contribute to the progression of OA in TMJ epigenetically. Significant hypomethylation of the GADD45 family genes, *Gadd45b* and *Gadd45g*, has also been identified at all three stages of TMJOA, which implicated in a variety of the responses to cell injury, physiological stress, including cell cycle checkpoints, apoptosis, and their proteins could promote active DNA demethylation thereby mediating gene activation (Salvador et al., 2013; Schafer 2013).

Finally, our comparative analysis revealed 62 differentially methylated and inversely expressed genes at early or late stages of TMJOA. In particular, *Chad*, *Id2* and *Mexo2*, were detected in both stages. Chondroadherin (*Chad*) is a cartilage matrix protein that has been shown to promote integrin$\alpha 2\beta 1$-mediated attachment of chondrocytes and fibroblasts (Haglund, Tillgren, & Addis, 2011). The upregulation of *Chad* expression observed in our microarray analysis was verified by real-time PCR. Inhibitor of DNA binding2 (*Id2*) plays a pivotal role in acting downstream of BMP signaling, to regulate cartilage formation during the postnatal stage (Sakata-Goto, Takahashi, & Kiso, 2012). Mesenchyme homeobox 2 (MEOX2) plays a role in mesoderm induction, somitogenesis and myogenic differentiation (Mankoo, Skuntz, & Harrigan, 2003); however, its specific functions in OA remain elusive.

In summary, as DNA methylation is a dynamic process influenced by environmental stimuli and age-related loss, the aim of the present study was to describe the first genome-scale DNA methylation profiles in three different stages of rat TMJOA. We demonstrated that different stages of TMJOA can be distinguished from the healthy mandibular head cartilage by their distinct DNA methylation patterns, and the group of differentially methylated genes and enriched pathways at the late stage support well the pathogenetic mechanisms epigenetically. Furthermore, we identified a group of continuously differentially methylated genes, typically *Cldn11* and *Chad*, and a set of biological processes and signal pathways, which are beneficial for the pathogenetic genes identification and further molecular investigations. Despite concerns regarding the relatively high number of CpG regions in our microarray and the epigenetic differences between rats and humans, these findings warrant further investigations of human TMJOA, including both *in vitro* and *in vivo* functional studies.

Funding

This study was supported by grants from the National Natural Science Foundation of China (31271548). The sponsors did not play any role in this study.

Conflict of interest

The authors declare no conflict of interest related to this study.

Ethical approval

This research was approved by the Peking University Institutional Animal Care and Use Committee.

Acknowledgments

We would like to thank Xian Peng Ge for suggestions to the design of our study, and Wei Ping Wang, Zhu Qing Jia for the technical assistance.

Appendix A. Supplementary data

Supplementary data associated with this article can be found, in the online version, at http://dx.doi.org/10.1016/j.archoralbio.2016.04.006.

References

Agarwal, R., Mori, Y., Cheng, Y., et al. (2009). Silencing of claudin-11 is associated with increased invasiveness of gastric cancer cells. *PLoS One*, *4*(11), e8002.

Al Moustafa, A. E., Alaoui-Jamali, M. A., Batist, G., et al. (2002). Identification of genes associated with head and neck carcinogenesis by cDNA microarray comparison between matched primary normal epithelial and squamous carcinoma cells. *Oncogene*, *21*(17), 2634–2640.

Barter, M. J., Bui, C., & Young, D. A. (2012). Epigenetic mechanisms in cartilage and osteoarthritis: DNA methylation, histone modifications and microRNAs. *Osteoarthritis and Cartilage*, *20*(5), 339–349.

Bergman, Y., & Cedar, H. (2013). DNA methylation dynamics in health and disease. *Nature Structural & Molecular Biology*, *20*(3), 274–281.

Bronstein, J. M., Chen, K., Tiwari-Woodruff, S., et al. (2000). Developmental expression of OSP/claudin-11. *Journal of Neuroscience Research*, *60*(3), 284–290.

Bronstein, J. M., Popper, P., Micevych, P. E., et al. (1996). Isolation and characterization of a novel oligodendrocyte-specific protein. *Neurology*, *47*(3), 772–778.

Cao, W., Liu, J., Xia, R., et al. (2016). X-linked FHL1 as a novel therapeutic target for head and neck squamous cell carcinoma. *Oncotarget*.

Cheung, K. S., Hashimoto, K., Yamada, N., et al. (2009). Expression of ADAMTS-4 by chondrocytes in the surface zone of human osteoarthritic cartilage is regulated by epigenetic DNA de-methylation. *Rheumatology International*, *29*(5), 525–534.

Dijkgraaf, L. C., de Bont, L. G., Boering, G., et al. (1995). The structure, biochemistry, and metabolism of osteoarthritic cartilage: a review of the literature. *Journal of Oral and Maxillofacial Surgery*, *53*(10), 1182–1192.

Esteller, M., Garcia-Foncillas, J., Andion, E., et al. (2000). Inactivation of the DNA-repair gene MGMT and the clinical response of gliomas to alkylating agents. *New England Journal of Medicine*, *343*(19), 1350–1354.

Fernandez-Tajes, J., Soto-Hermida, A., Vazquez-Mosquera, M. E., et al. (2014). Genome-wide DNA methylation analysis of articular chondrocytes reveals a cluster of osteoarthritic patients. *Annals of the Rheumatic Diseases*, *73*(4), 668–677.

Gao, L., van den Hurk, K., Moerkerk, P. T., et al. (2014). Promoter CpG island hypermethylation in dysplastic nevus and melanoma: CLDN11 as an epigenetic biomarker for malignancy. *The Journal of Investigative Dermatology*, *134*(12), 2957–2966.

Gepstein, A., Shapiro, S., Arbel, G., et al. (2002). Expression of matrix metalloproteinases in articular cartilage of temporomandibular and knee joints of mice during growth, maturation, and aging. *Arthritis and Rheumatism*, *46*(12), 3240–3250.

Haglund, L., Tillgren, V., Addis, L., et al. (2011). Identification and characterization of the integrin alpha2beta1 binding motif in chondroadherin mediating cell attachment. *The Journal of Biological Chemistry*, *286*(5), 3925–3934.

Huang, K., & Wu, L. D. (2008). Aggrecanase and aggrecan degradation in osteoarthritis: a review. *The Journal of International Medical Research*, *36*(6), 1149–1160.

Huang da, W., Sherman, B. T., & Lempicki, R. A. (2009). Systematic and integrative analysis of large gene lists using DAVID bioinformatics resources. *Nature Protocols*, *4*(1), 44–57.

Ikeda, Y., Yonemitsu, I., Takei, M., et al. (2014). Mechanical loading leads to osteoarthritis-like changes in the hypofunctional temporomandibular joint in rats. *Archives of Oral Biology*, *59*(12), 1368–1376.

Jeffries, M. A., Donica, M., Baker, L. W., et al. (2014). Genome-wide DNA methylation study identifies significant epigenomic changes in osteoarthritic cartilage. *Arthritis & Rheumatology*, *66*(10), 2804–2815.

Jiao, K., Niu, L. N., Wang, M. Q., et al. (2011). Subchondral bone loss following orthodontically induced cartilage degradation in the mandibular condyles of rats. *Bone*, *48*(2), 362–371.

Kalladka, M., Quek, S., Heir, G., et al. (2014). Temporomandibular joint osteoarthritis: diagnosis and long-term conservative management: a topic review. *Journal of Indian Prosthodontic Society*, *14*(1), 6–15.

Kominsky, S. L., Argani, P., Korz, D., et al. (2003). Loss of the tight junction protein claudin-7 correlates with histological grade in both ductal carcinoma in situ and invasive ductal carcinoma of the breast. *Oncogene*, *22*(13), 2021–2033.

Komori, T. (2005). Regulation of skeletal development by the Runx family of transcription factors. *Journal of Cellular Biochemistry*, *95*(3), 445–453.

Lekkas, C., Honee, G. L., & van den Hooff, A. (1988). Effects of experimental defects of the articular disc of the temporomandibular joint in rats. *Journal of Oral Rehabilitation*, *15*(2), 141–148.

Li, W., Wu, M., Jiang, S., et al. (2014). Expression of ADAMTs-5 and TIMP-3 in the condylar cartilage of rats induced by experimentally created osteoarthritis. *Archives of Oral Biology*, *59*(5), 524–529.

Mankoo, B. S., Skuntz, S., Harrigan, I., et al. (2003). The concerted action of Meox homeobox genes is required upstream of genetic pathways essential for the formation, patterning and differentiation of somites. *Development*, *130*(19), 4655–4664.

Meng, J., Ma, X., Ma, D., et al. (2005). Microarray analysis of differential gene expression in temporomandibular joint condylar cartilage after experimentally induced osteoarthritis. *Osteoarthritis and Cartilage*, *13*(12), 1115–1125.

Morgan, H. D., Santos, F., Green, K., et al. (2005). Epigenetic reprogramming in mammals. *Human Molecular Genetics*, *14*(1), R47–R58.

Nampei, A., Hashimoto, J., Hayashida, K., et al. (2004). Matrix extracellular phosphoglycoprotein (MEPE) is highly expressed in osteocytes in human bone. *Journal of Bone and Mineral Metabolism*, *22*(3), 176–184.

Nichols, L. S., Ashfaq, R., & Iacobuzio-Donahue, C. A. (2004). Claudin 4 protein expression in primary and metastatic pancreatic cancer: support for use as a therapeutic target. *American Journal of Clinical Pathology*, *121*(2), 226–230.

Niu, S. P., Huang, C. B., Zhao, L. K., et al. (2011). The role of promoter CpG islands methylation of leptin gene in osteoarthritis. *Zhonghua nei ke za zhi*, *50*(1), 55–58.

Palmke, N., Santacruz, D., & Walter, J. (2011). Comprehensive analysis of DNA-methylation in mammalian tissues using MeDIP-chip. *Methods*, *53*(2), 175–184.

Pelizzola, M., Koga, Y., Urban, A. E., et al. (2008). MEDME: an experimental and analytical methodology for the estimation of DNA methylation levels based on microarray derived MeDIP-enrichment. *Genome Research*, *18*(10), 1652–1659.

Prasadam, I., Crawford, R., & Xiao, Y. (2012). Aggravation of ADAMTS and matrix metalloproteinase production and role of ERK1/2 pathway in the interaction of osteoarthritic subchondral bone osteoblasts and articular cartilage chondrocytes—possible pathogenic role in osteoarthritis. *The Journal of Rheumatology*, *39*(3), 621–634.

Probert, L., Akassoglou, K., Alexopoulou, L., et al. (1996). Dissection of the pathologies induced by transmembrane and wild-type tumor necrosis factor in transgenic mice. *Journal of Leukocyte Biology*, *59*(4), 518–525.

Ramasamy, S. K., Kusumbe, A. P., Wang, L., et al. (2014). Endothelial Notch activity promotes angiogenesis and osteogenesis in bone. *Nature*, *507*(7492), 376–380.

Reynard, L. N., Bui, C., Canty-Laird, E. G., et al. (2011). Expression of the osteoarthritis-associated gene GDF5 is modulated epigenetically by DNA methylation. *Human Molecular Genetics*, *20*(17), 3450–3460.

Reynard, L. N., & Loughlin, J. (2012). Genetics and epigenetics of osteoarthritis. *Maturitas*, *71*(3), 200–204.

Ritchie, M. E., Phipson, B., Wu, D., et al. (2015). limma powers differential expression analyses for RNA-sequencing and microarray studies. *Nucleic Acids Research*, *43*(7), e47.

Roach, H. I., Yamada, N., Cheung, K. S., et al. (2005). Association between the abnormal expression of matrix-degrading enzymes by human osteoarthritic chondrocytes and demethylation of specific CpG sites in the promoter regions. *Arthritis and Rheumatism*, *52*(10), 3110–3124.

Rushton, M. D., Reynard, L. N., Barter, M. J., et al. (2014). Characterization of the cartilage DNA methylome in knee and hip osteoarthritis. *Arthritis & Rheumatology*, *66*(9), 2450–2460.

Sakata-Goto, T., Takahashi, K., Kiso, H., et al. (2012). Id2 controls chondrogenesis acting downstream of BMP signaling during maxillary morphogenesis. *Bone*, *50*(1), 69–78.

Salvador, J. M., Brown-Clay, J. D., & Fornace, A. J. Jr. (2013). Gadd45 in stress signaling, cell cycle control: and apoptosis. *Advances in Experimental Medicine and Biology*, *793*, 1–19.

Schafer, A. (2013). Gadd45 proteins: key players of repair-mediated DNA demethylation. *Advances in Experimental Medicine and Biology*, *793*, 35–50.

Schubeler, D. (2015). Function and information content of DNA methylation. *Nature*, *517*(7534), 321–326.

Tanaka, E., Detamore, M. S., & Mercuri, L. G. (2008). Degenerative disorders of the temporomandibular joint: etiology, diagnosis, and treatment. *Journal of Dental Research*, *87*(4), 296–307.

Toedling, J., Skylar, O., Krueger, T., et al. (2007). Ringo—an R/Bioconductor package for analyzing ChIP-chip readouts. *BMC Bioinformatics*, *8*, 221.

Weber, M., Davies, J. J., Wittig, D., et al. (2005). Chromosome-wide and promoter-specific analyses identify sites of differential DNA methylation in normal and transformed human cells. *Nature Genetics*, *37*(8), 853–862.

Yano, F., Hojo, H., Ohba, S., et al. (2013). A novel disease-modifying osteoarthritis drug candidate targeting Runx1. *Annals of the Rheumatic Diseases*, *72*(5), 748–753.